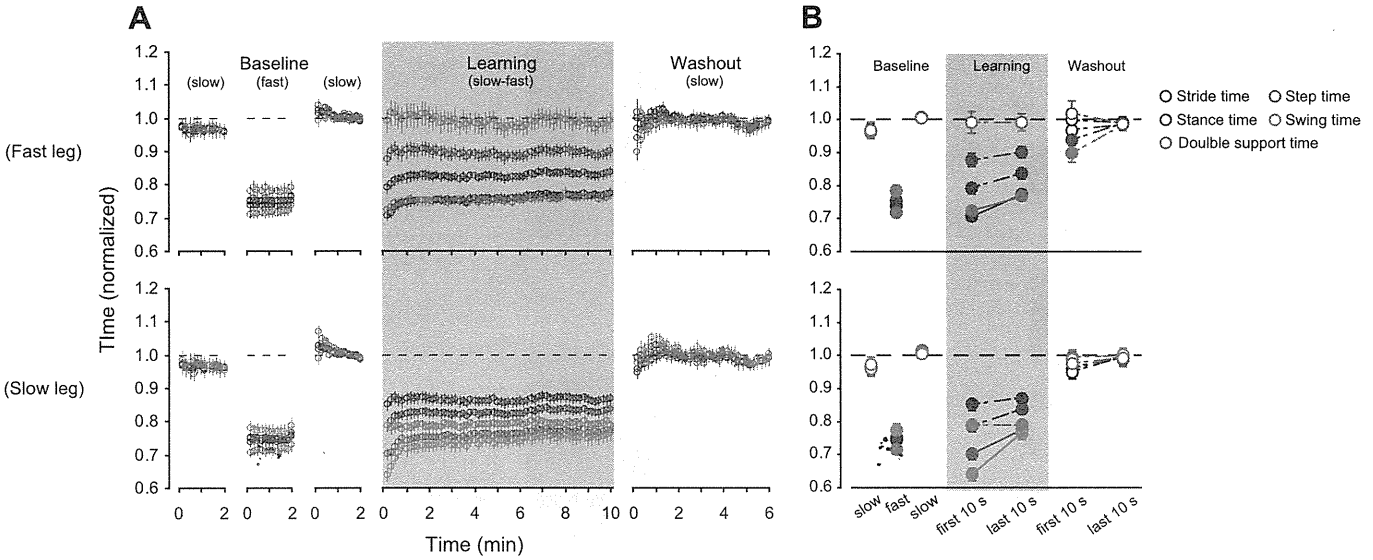

Fig. 2. *A*: mean of the time series changes of the temporal parameters for the whole experimental protocol (fast leg on the *top row* and slow leg on the *bottom row*). *B*: comparisons of each parameter at different time points. All the data were normalized to those of the baseline (for details, see METHODS). Filled circles indicate statistically significant differences from those during the baseline period, and the solid lines show the significant differences between the variables. Error bars indicate means ± SE. Differences were considered statistically significant when $P < 0.05$.

differences the changes could be categorized into three different patterns. The results are described in Fig. 3 for the whole experimental protocol (*left*) and for the comparison among different time points (*right*) to address the capability of adaptation. Figure 3, *middle*, highlights the first part of each learning and washout periods. At the beginning of the adaptation period, the mediolateral and the posterior components (*A* and *D*) of GRF showed significant deviations from the baseline at the beginning of split-belt period in both the slow ($P < 0.05$ for mediolateral, and $P < 0.01$ for posterior) and the fast leg ($P < 0.001$ for mediolateral, and $P < 0.001$ for posterior). Here, the slow leg values were adjusted to be near those in the slow baseline and the fast leg values were adjusted to be near those in the fast baseline. In the adaptation period, the mediolateral component in the fast leg gradually decreased toward the fast baseline values after initial overshoot. The comparison between the first and last 10 s of the adaptation period showed a significant difference ($P < 0.05$). The other comparisons did not show such a change. Upon return to the tied belt condition, there were significant aftereffects in the fast ($P < 0.01$) and slow ($P < 0.01$) legs in the mediolateral component and only in the slow leg in the posterior component ($P < 0.05$). The vertical component, on the other hand (Fig. 3*B*), showed somewhat different behavior from the mediolateral or the posterior components described above. At the beginning of the adaptation period, the relationship between the values for the fast leg and those for the slow leg were flipped from the baseline values (the fast leg values approached the slow baseline values and the slow leg values approached the fast baseline values). Only the slow leg showed significant deviation from the baseline initially ($P < 0.01$), and it did not exhibit any capability of adaptation during the 10-min test period. There were no evident aftereffects in either the fast or slow legs in this component.

Among the four different components of the GRF, the anterior component showed the clearest signs of adaptation and washout in both legs (Fig. 3*C*). At the initial stage of the adaptation period, the mean value in the fast leg was adjusted to be close to the slow baseline value, whereas in the slow leg ($P < 0.001$) it was near the value of the fast baseline period. There were steep changes in the first min followed by moderate changes lasting for the remaining 9 min during the adaptation period, where the relationship between the legs flipped early in the period. At the completion of the adaptation period, the value in the fast leg was adjusted to be close to that of the fast baseline and the value in the slow leg was adjusted to be close to that of the slow baseline. There were significant differences between the first and last 10 s in both the fast ($P < 0.001$) and slow ($P < 0.001$) legs. The washout phase started with pronounced deviation from the baseline in both legs, and there were gradual changes toward the baseline values, with the overall pattern of change into the opposite direction to that during the adaptation period. The statistical comparisons demonstrated significant deviation from the baseline at the beginning of the washout phase [$P < 0.001$ (fast) and $P < 0.01$ (slow)] and differences between the initial and the last 10 s in the washout in both the fast ($P < 0.001$) and slow ($P < 0.01$) legs.

EMG responses. Figure 4 shows the time series changes in the EMG activity for the whole experimental protocol (*left*) and for the comparison among different time points at selected time periods during the stance and the swing phases (*right*). Generally, the EMG responses were more variable than were the temporal parameters and ground reaction force data.

During the initial stage of the adaptation period, activities in the BF muscle in the fast leg and the RF and TA muscles in the slow leg increased during the stance phase. The activity of these muscles exhibited a clear adaptive curve, with the values gradually decreasing toward the baseline values. At 10 min, the values were almost identical to the baseline values, despite the fact that the subject was walking on a split treadmill surface. The statistical comparison revealed in those muscles that there were initially significant differences from the baseline values [$P < 0.001$ (fast BF), $P < 0.001$ (slow RF), and $P < 0.01$

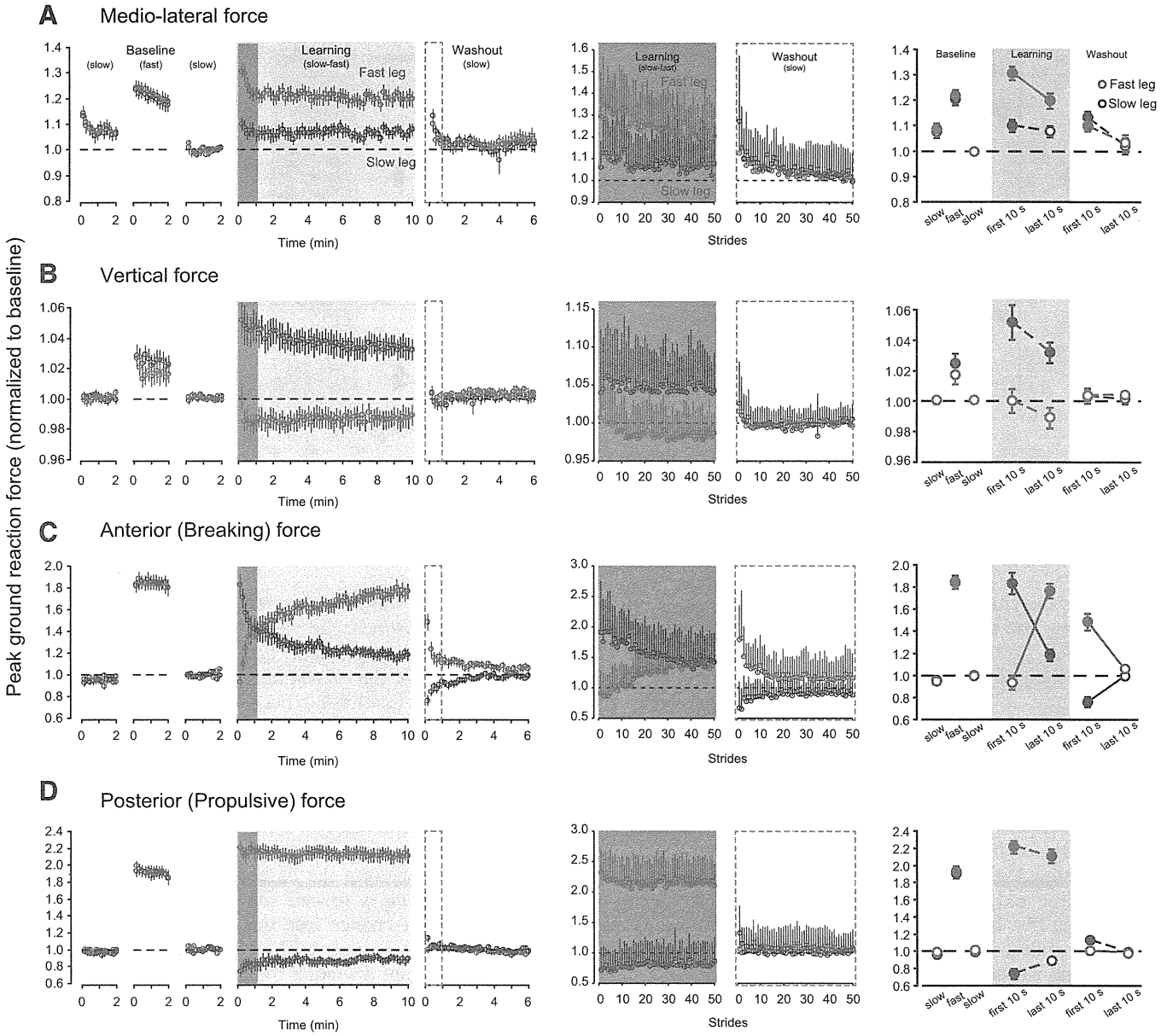

Fig. 3. Time series changes of the GRF components. (*A*: lateral; *B*: vertical; *C*: anterior; *D*: posterior). Blue circles are the values for the slow leg under the "adaptation" period, and the red circles indicate those of the fast leg. Averaged value of each 10-s bin are shown at *left*, and each step data at the beginning of adaptation and washout periods (first 50 steps) are shown at *middle*. *Right*: comparisons of each parameter at different time points. All the data were normalized to those of the baseline values (for details, see METHODS). Filled circles indicate statistically significant differences from those during the baseline period, and the solid lines show the significant differences between the variables. Error bars indicate means ± SE. Differences were considered statistically significant when $P < 0.05$.

(slow TA)]. There were also statistically significant differences in these muscles between the initial and final 10 s in the 10-min adaptation phase, demonstrating the capability of adaptation [$P < 0.001$ (fast BF), $P < 0.001$ (slow RF), and $P < 0.01$ (slow TA)]. With the return to the tied belt condition, the TA, RF, and BF muscles in the fast leg and the MG and RF muscles in the slow leg showed augmented activity. Although the belt condition was identical to that in the baseline period, the EMG activities were significantly different from those in the baseline period [$P < 0.05$ (fast TA), $P < 0.01$ (fast RF), $P < 0.01$ (fast BF), $P < 0.01$ (slow MG), and $P < 0.05$ (slow RF)]. These activities gradually decreased toward the baseline level within the first 2 min or so. Around 5 min in the washout phase, the levels of these activities were similar to the baseline values.

During the swing phase, the TA ($P < 0.01$) and BF ($P < 0.01$) muscles in the fast leg and RF muscle in the slow leg ($P < 0.05$) showed augmented activities in the early adaptation period compared with those at baseline, where only the BF in the fast leg ($P < 0.05$) and the RF in the slow leg ($P < 0.05$) exhibited a clear pattern of adaptation. In the following washout period, only the BF muscle showed an initial enhancement of the activity ($P < 0.01$) and a pattern of washout ($P < 0.001$) toward the baseline level. In the RF muscles of the fast limb, the activities were lessened even below baseline levels ~5 min

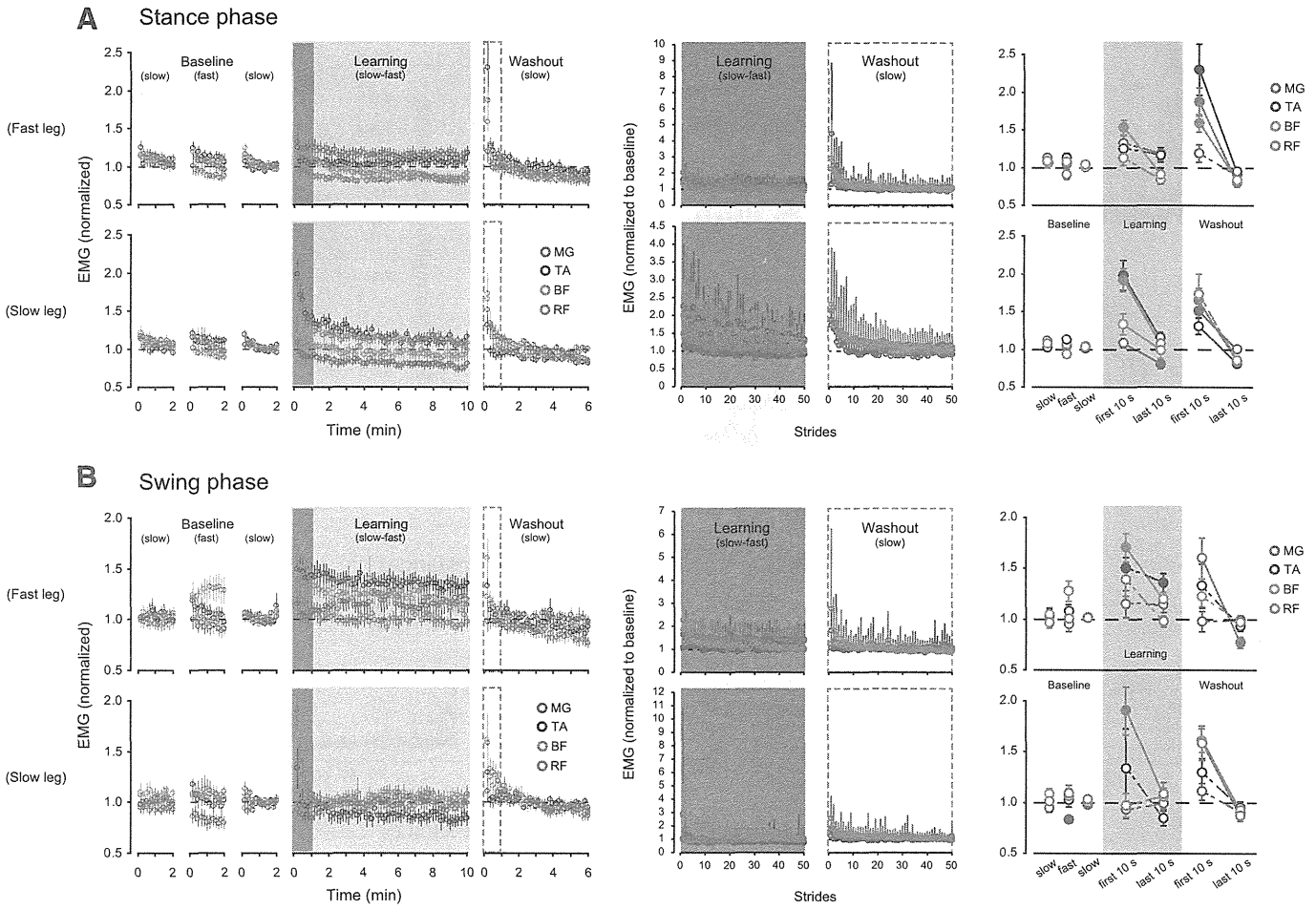

Fig. 4. *A* and *C*: mean of the time series changes of the EMG activities in each muscle investigated during the stance phase (*A*) and the swing phase (*C*). All the data were normalized to those under the baseline condition. *Top rows*: activities of the fast leg during the adaptation period, and the data in the lower rows are those of the slow leg. *B* and *D*: comparisons of the mean values at different time points. Filled circles indicate statistically significant differences from those during the baseline period, and the solid lines show the significant differences between the variable. Error bars indicate means ± SE. Differences were considered statistically significant when $P < 0.05$.

in the washout period ($P < 0.01$), and the reductions resulted in statistically significant differences between the initial and final 10 s of the period in both legs [$P < 0.01$ (fast) and $P < 0.01$ (slow)].

In contrast to the TA muscles during the stance phase (initially increased activity and subsequent decrement in the slow leg during the adaptation period and the emergence of the aftereffect in the fast leg), the activities in the MG exhibited contrastive behavior. Figure 5*A* presents representative EMG waveforms in the TA and MG muscles under stride cycles at different time points of the experiment. Figure 5*B* highlights a distinct adaptive process between the slow (blue) and fast (red) legs of the TA EMG in the early stance phase and the MG EMG in the late stance phase. At the initial stage of the adaptation period, the TA EMG in the slow leg showed higher values, and then at the completion of the adaptation period, the values in the fast leg were adjusted to be close to those of the fast baseline and the values in the slow leg were adjusted to be close to those of the slow baseline.

The washout phase started with a pronounced deviation from the baseline in the fast leg, and there were gradual changes toward the baseline values. In contrast to the TA muscle, only the slow leg showed significant deviation from the baseline initially ($P < 0.01$), and it did not exhibit any capability of adaptation during the 10-min test period in the MG muscle. In the washout period, both legs showed higher values and then gradually recovered to the baseline values. Figure 5*C* focuses on the EMG activity under particular phases and in particular muscles where activity is essential for functional gait, that is, the mean EMG activity of the TA muscle during the early stance phase and that of the MG muscle during the late stance phase. A pattern of adaptation and subsequent aftereffects with relatively longer time course is found in the TA muscle ($P < 0.01$ to the baseline in the early adaptation period and $P < 0.01$ between early and late adaptation periods in the slow leg, and $P < 0.05$ to the baseline in the early washout period and $P < 0.05$ between early and late washout periods in the fast leg), while such activities are less evident in the MG muscle.

Figure 5*D* shows the relationship between the extent of adaptation of the slow/fast leg and the washout of contralateral leg in each TA/MG muscle, respectively (*top/bottom*). The regression line and the correlation coefficient value and its significance are indicated in the figure. A significant positive correlation was found in both muscles ($P < 0.05$), suggesting that the EMG patterns obtained on one side in the adaptation

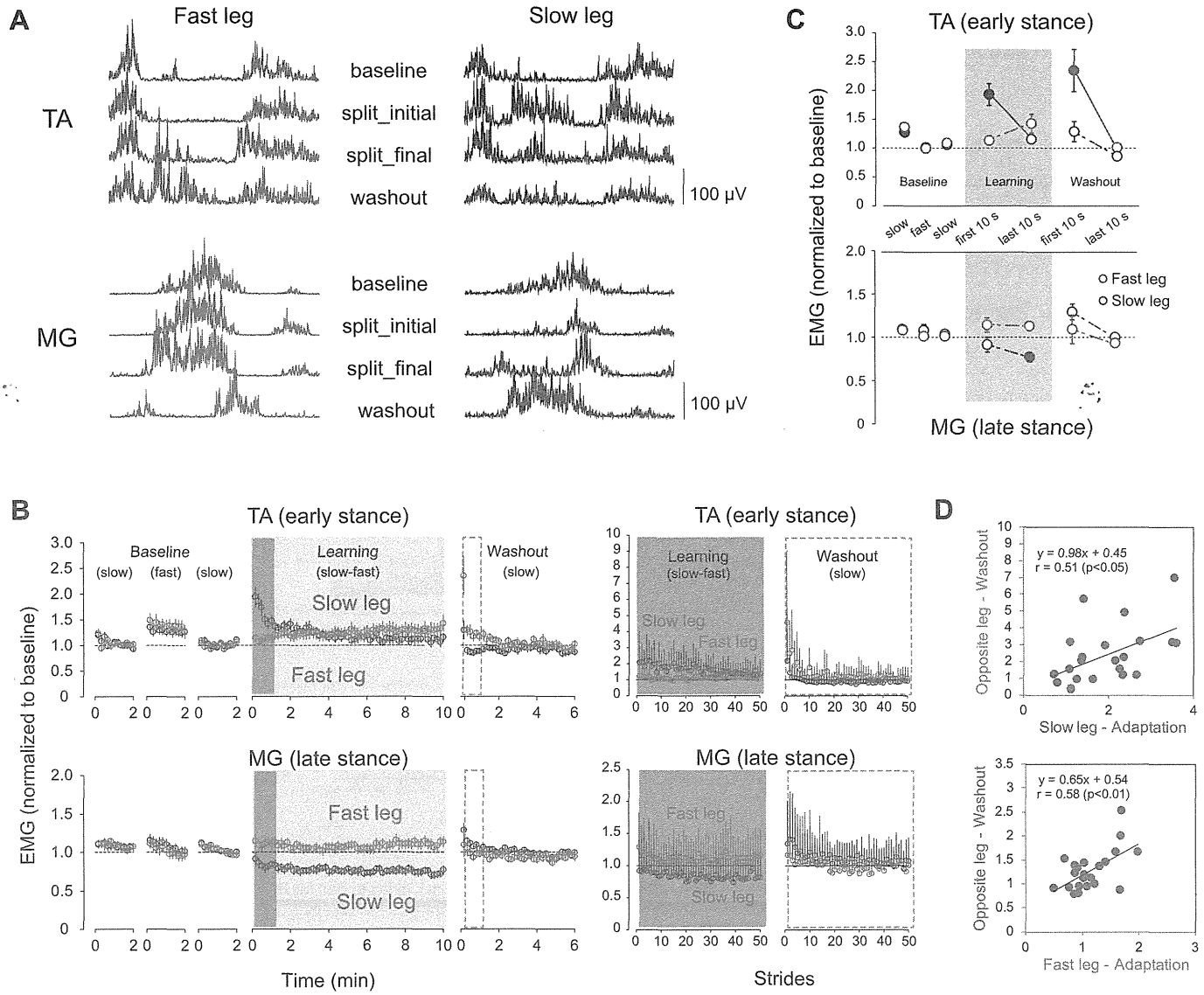

Fig. 5. *A*: representative waveforms of the EMG activities in the TA and MG muscles for both the fast and slow legs (those on the fast and slow belts during the adaptation period, respectively) at different time points. Each waveform represents an ensemble average of five consecutive stride cycles under the respective time points and is time normalized to stride cycles. *B*: mean of the time series changes of the EMG activities in the TA muscle during the first half of the stance phase and in the MG muscle during the last half of the stance phase. Filled circles represent the EMG activities during the first half of each gait cycle, and the open circles are those of the last half of the gait cycle. Averaged value of each 10 s bin are shown at *left*, and each step data at the beginning of adaptation and washout periods (first 50 steps) are shown at *right*. *C*: comparisons of each parameter at different time points (*top*: early stance of TA; *bottom*: late stance of MG). All the data were normalized to those of the baseline values (for details, see METHODS). Filled circles indicate statistically significant differences from those during the baseline period, and the solid lines show the significant differences between the variables. Error bars indicate means ± SE. Differences were considered significant at $P < 0.05$. *D*: relationship between the extent of adaptation of the slow/fast leg and the washout of the contralateral leg in the TA/MG muscle, respectively (*top/bottom*). Regression lines and the correlation coefficients and their significance are indicated in *A–D*.

period and the other side in the washout period switched with each other.

Relationship between the different variables. Figure 6 illustrates the relationship between the extent of adaptation and aftereffects for each variable (EMG_MG, EMG_TA, GRF_Braking, GRF_Propulsive). In the TA muscle, a positive correlation between adaptation and aftereffects was found in the fast leg (fast leg: $r = 0.429$, $P < 0.05$, slow leg: $r = 0.29$, n.s.). In the MG muscle, both the fast and slow legs showed a positive correlation between adaptation and aftereffects (fast leg: $r = 0.755$, $P < 0.05$, slow leg: $r = 0.446$, $P < 0.05$). Regarding the GRF data, a significant negative correlation was found only in the braking force of the slow leg (fast leg: $r = -0.180$, n.s., slow leg: $r = -0.459$, $P < 0.05$). No significant correlation was found in propulsive force in both legs (fast leg: $r = -0.064$, n.s., slow leg: $r = -0.159$, n.s.).

Tied-random (control) condition. Figure 7 shows the time series changes of the step time, braking GRF, and EMG activity in TA and MG muscles during the tied-random condition and the split-belt treadmill condition. The tied-random condition did not show any aftereffect in the postperturbation period, whereas the split-belt treadmill condition showed clear aftereffects in the washout period.

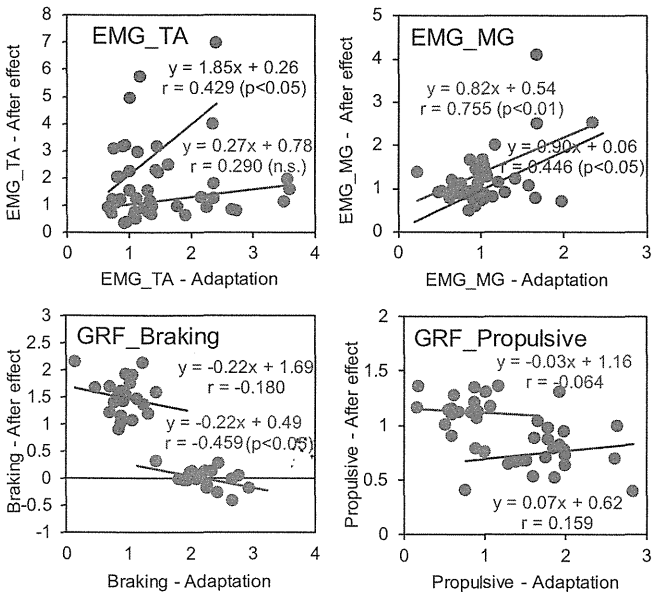

Fig. 6. Relationship between the extent of adaptation and washout for each variable (EMG_MG, EMG_TA, GRF_Braking, GRF_Propulsive). Regression lines and the correlation coefficients and their significance are indicated.

DISCUSSION

The purpose of this study was to elucidate the role of predictive and reactive feedback strategies during locomotor adaptations to split-belt treadmill walking. In the present study, we followed an experimental protocol used in Reisman et al. (2005), which was the first systematic study in a series of studies on split-belt treadmill adaptation. As clearly shown in the Fig. 3, the anterior component of the GRF showed a clear pattern of adaptation and subsequent aftereffects. Namely, the slow leg, through learning to walk on the slower belt, initially showed a significant increase in the braking force followed by a gradual decrease during the adaptation period, and then an abrupt reduction in the initial phase of washout. In contrast, the posterior component of GRF (propulsive force) showed a consistent increase/decrease in the fast/slow leg during the adaptation period and was not followed by subsequent aftereffects. The contrasting results between the braking and propulsive forces might reflect the existence of distinct control strategies underlying split-belt locomotor adaptation. The results obtained from lower limb EMG muscle also demonstrated a unique pattern due to the split-belt treadmill adaptation. In the following section, the detailed mechanisms underlying the split-belt treadmill adaptation and implications for the future use of the split-belt treadmill adaptation will be discussed.

Two distinct strategies underlying split-belt treadmill adaptation. The emergence of the adaptive and the subsequent de-adaptive phenomena with and after walking on a split-belt treadmill has been studied extensively by Bastian and colleagues over the last decade (Reisman et al. 2005, 2007, 2009; Morton and Bastian 2006; Choi et al. 2007, 2009; Vasudevan and Bastian 2010; Malone and Bastian 2010; Torres-Oviedo and Bastian 2010; Vasudevan et al. 2011; Musselman et al. 2011). Based on a series of split-belt treadmill experiments, Bastian and colleagues clearly dissociated different forms of locomotor adaptation, reactive and predictive adjustments, in the central nervous system. However, the details of the specific gait pattern adjustments made by subjects on an asymmetrically driven split-belt treadmill were not fully understood.

The novel contribution of the present study is to provide the specific patterns of the predictive feedforward and reactive feedback control strategies based on the GRF and EMG results. As clearly shown in the Fig. 3, the anterior component of the GRF in slow leg showed a clear pattern of adaptation and subsequent aftereffects, which is comparable to those originally identified in the reaching movement of the upper arm, which is the process for the recalibration of motor command with the new task demand (Kawato et al. 1987; Shadmehr and Mussa-Ivaldi 1994). Although the type of movement differs between upper limb motion and bipedal walking, adaptation to the split-belt treadmill can also be regarded as a process of trial-and-error-based adjustment of gait behavior in response to differently driven belts. At the initial part of split-belt walking, the central nervous system does not correctly predict the extent of perturbation and causal postural disturbance (movement error) due to the split belts. With continuous exposure to the split-belt condition, the subjects could finally establish the predictive feedforward motor command that enabled them to minimize the extent of postural disturbance presented by the split-belt condition.

Concerning this point, the authors of previous studies suggested the significance of feedforward mechanisms in human locomotion by comparing specific muscle activity during an "adapted state" in an imposed force field and upon the unexpected removal of the force field with the use of gait robotics (Lam et al. 2006) and an elastic band (Blanchette and Bouyer 2009). Taking the present results into account together with these previous findings, it is likely that the process comprising the braking force can be regarded as a predictive feedforward component of the motor control for bipedal walking. Given the importance of cerebellar function for acquiring the predictive feedforward model (Imamizu et al. 2000; Bastian 2006), similar neural processes might be involved in the split-belt treadmill adaptation.

In contrast, the posterior GRF showed a consistent increase/decrease in the fast/slow leg during the adaptation period and was not followed by subsequent aftereffects, suggesting that propulsive force can be regarded as the result of reactive adjustment which is presumably generated by an automatic feedback action. The manner of changes between anterior and posterior forces might reflect the existence of distinct control strategies underlying split-belt locomotor adaptation. We next discuss the possible mechanisms underlying GRF results based on our measurement of EMG activity.

Different role of each limb for accomplishing split-belt treadmill adaptation. In light of the asymmetrically driven support surface used in the present study, we suspect that the slow and fast legs have different functional roles for the accomplishment of gait adaptation. As indicated above, control of the braking force might involve an error-based learning process. Importantly, slower side plays a significant role as a "reference" for adaptation to walk normally under the novel circumstance of moving on an asymmetrically driven split-belt treadmill. Higher vertical GRF in the slow leg during the adaptation period also reflects that the subject tended to put much weight on this side.

As shown in Fig. 6, while the fast and slow legs show similar relationships between the extent of adaptation and the subse-

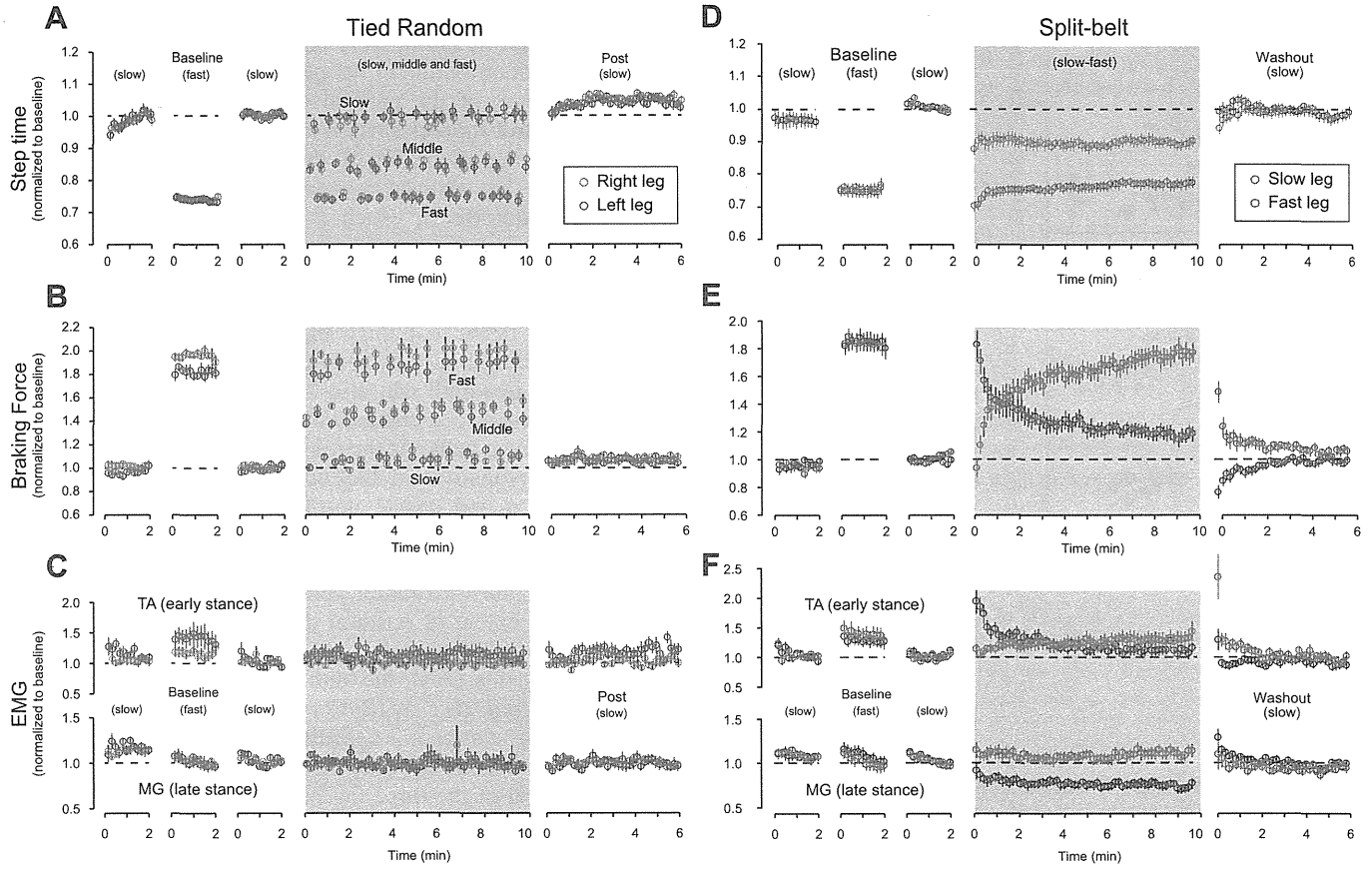

Fig. 7. Time series changes of the step time (*A* and *D*), braking GRF (*B* and *E*), and EMG activity in the TA and MG muscles (*C* and *F*) during the tied-random condition (*left*) and the split-belt treadmill condition (*right*). *Left*: cyan and magenta circles are the values for the right and left leg, respectively. *Right*: blue and red circles are the values for the slow and fast legs during the split-belt condition, respectively. Averaged values of each 10-s bin are shown. All data were normalized to those of the baseline values.

quent aftereffects in the EMG activity of the MG muscle, other parameters showed a clear difference between the slow (blue) and fast leg (red). These results also suggested different roles of each leg in split-belt adaptation. These interpretations are in agreement with the previous study stated that the slow moving leg was used as the primary support to stabilize the body equilibrium during the prolonged swing of the contralateral leg (Dietz et al. 1994; Duysens et al. 2004). Moreover, our results are in line with the previous report that the emergence of aftereffects after walking on an asymmetrically driven treadmill surface was always merged with a speed identical to that of the slower side during the adaptation periods (Vasudevan et al. 2010).

In addition to the contrasting braking force results between the fast and slow legs, other GRF parameters also showed remarkable differences between the legs, e.g., the larger shift of the lateral GRF and the enhancement of propulsive force in the fast leg. These results might reflect the larger amount of perturbation in the fast leg during the stance phase of walking. It is noteworthy that lateral GRF in the fast leg showed some extent of adaptation and subsequent aftereffect. The adaptive changes observed in the lateral and braking forces suggest that the maintenance of balance would be one of the necessary outcomes to achieve stable walking in the split-belt condition. Regarding this point, Finley et al. (2013) revealed that acquisition of an economical movement pattern is an important element of locomotor adaptation to novel environments. The reduction in metabolic power might be relevant to acquired stable walking as the result of split-belt treadmill adaptation.

Detail mechanisms underlying split-belt adaptation. As shown in Fig. 4, EMG responses in the TA, RF, and BF muscles during the stance phase and the BF muscle during the swing phase showed clear adaptive and de-adaptive processes. Most interestingly, the time series changes of the muscle activity in the TA muscles, especially during the early stance phase, resembled those of the braking force (Figs. 3 and 5). Duysens et al. (2004) also reported that the TA muscle remains active throughout most of the stance phase of the slow moving leg during split-belt treadmill walking. They interpreted this inadvertent activity as a result of coactivation of agonistic and antagonistic leg muscles to stabilize body equilibrium during the prolonged swing of the contralateral leg.

The TA muscle is typically activated from the beginning of the leg swing to the early stance phase. The abovementioned coactivation period at the early stance phase might be functionally essential to stabilize the ankle joint securely soon after a heel strike (Nakazawa et al. 2004). During split-belt treadmill walking, adjustment of the ankle stiffness in response to split-belt-induced perturbation is quite important. In addition, the subject might learn a causal relationship between the extent of perturbation and optimal ankle stiffness by an error-based learning process during the adaptation period, and they may

finally acquire predictive control of the ankle stiffness at the heel contact.

Regarding the control of ankle stiffness in the early stance phase during walking, it was demonstrated that a significantly large motor-evoked potential (Capaday et al. 1999) and long-latency stretch reflex (Christensen et al. 2000) are induced in the TA muscle at the early stance during walking. These findings strongly suggested that the enhancement of the excitability of TA corticospinal and stretch reflex pathways is necessary as an action to prepare for the upcoming perturbation at the heel contact. In light of these findings, it is likely that the total involvement of the cortical process is relatively larger at the beginning of adaptation to the split-belt-induced perturbation and, then, error-based learning enables the subject to update the internal model for walking, which presumably takes place in the cerebellum (Morton and Bastian 2006, Jayaram et al. 2012).

It might be speculated that the adaptation and subsequent aftereffects observed in split-belt treadmill walking are due merely to the difficulty of treadmill walking because some parameters showed gradual changes even during the baseline period. It is thus necessary to discuss the process of the induction of a learning effect due to split-belt treadmill walking. To investigate this matter, we conducted a supplemental experiment in 10 subjects with a protocol similar to that employed by Jayaram et al. (2011) using a protocol where the belts are tied the entire time but the speeds are frequently varied (every 10 s). Although the total duration and walking distance in this experimental condition were similar between the tied-random and split-belt treadmill walking, the tied-random condition did not show any aftereffect in the postperturbation period (Fig. 7).

This result suggests that the adjustment of gait behavior in response to bilateral belt speed changes does not require any updating process of the internal model for walking. During the tied-random condition, the subjects needed only a few steps to adjust their walking stability after the belt speed change. This is because humans can adjust their walking by using an automatically induced reflex system utilizing sensory feedback and previous experience. However, the split-belt treadmill-induced perturbation is unusual, and no prior experience can be used as a template for gait adjustment. As a result, the subjects achieved stable walking by their trial-and-error-based learning.

Conclusion and implication. The present results regarding GRF and muscle EMG activities provide useful information for discussions of the motor control and learning process during split-belt adaptation and subsequent aftereffects. Our findings indicate that predictive feedforward control is required to set optimal ankle stiffness in preparation for the impact at the heel contact, and passive feedback control is utilized for the production of reflexively induced propulsive force at the end of the stance phase during split-belt treadmill adaptation. This conclusion might have direct implications for the construction of specific rehabilitation protocols for the improvement of gait asymmetry in poststroke patients. It is plausible that interventions using a split-belt treadmill have the potential to make systematic adjustments of imbalances between breaking and propulsive forces and asymmetry between paretic and intact legs.

GRANTS

This work was supported by Grant-in-Aid for Young Scientists (A) (#22680045) to N. Kawashima and Grant-in-Aid for Young Scientists (B) to T. Ogawa (Research Project Number: 23700658) from Japan Society for the Promotion of Science.

DISCLOSURES

No conflicts of interest, financial or otherwise, are declared by the author(s).

AUTHOR CONTRIBUTIONS

Author contributions: T. Ogawa and N.K. performed experiments; T. Ogawa and N.K. analyzed data; T. Ogawa and N.K. interpreted results of experiments; T. Ogawa and N.K. prepared figures; T. Ogawa and N.K. drafted manuscript; N.K. conception and design of research; N.K. edited and revised manuscript; N.K., T. Ogata, and K.N. approved final version of manuscript.

REFERENCES

Bastian AJ. Learning to predict the future: the cerebellum adapts feedforward movement control. *Curr Opin Neurobiol* 16: 645–649, 2006.

Blanchette A, Bouyer LJ. Timing-specific transfer of adapted muscle activity after walking in an elastic force field. *J Neurophysiol* 102: 568–577, 2009.

Bowden MG, Balasubramanian CK, Neptune RR, Kautz SA. Anterior-posterior ground reaction forces as a measure of paretic leg contribution in hemiparetic walking. *Stroke* 37: 872–876, 2006.

Capaday C, Lavoie BA, Barbeau H, Schneider C, Bonnard M. Studies on the corticospinal control of human walking. I. Responses to focal transcranial magnetic stimulation of the motor cortex. *J Neurophysiol* 81: 129–139, 1999.

Choi JT, Bastian AJ. Adaptation reveals independent control networks for human walking. *Nat Neurosci* 10: 1055–1062, 2007.

Choi JT, Vining EP, Reisman DS, Bastian AJ. Walking flexibility after hemispherectomy: split-belt treadmill adaptation and feedback control. *Brain* 132: 722–33, 2009.

Christensen LO, Petersen N, Andersen JB, Sinkjaer T, Nielsen JB. Evidence for transcortical reflex pathways in the lower limb of man. *Prog Neurobiol* 62: 251–272, 2000.

Dietz V, Zijlstra W, Duysens J. Human neuronal interlimb coordination during split-belt locomotion. *Exp Brain Res* 101: 513–520, 1994.

Dietz V. Human neural control of automatic functional movement. *Physiol Rev* 71: 33–58, 1992.

Duysens J, Bastiaanse CM, Smits-Engelsman BC, Dietz V. Gait acts as a gate for reflexes from the foot. *Can J Physiol Pharmacol* 82: 715–722, 2004.

Finley JM, Bastian AJ, Gottschall JS. Learning to be economical: the energy cost of walking tracks motor adaptation. *J Physiol* 591: 1081–1095, 2013.

Jayaram G, Galea JM, Bastian AJ, Celnik P. Human locomotor adaptive learning is proportional to depression of cerebellar excitability. *Cereb Cortex* 21: 1901–1909, 2011.

Imamizu H, Miyauchi S, Tamada T, Sasaki Y, Takino R, Pütz B, Yoshioka T, Kawato M. Human cerebellar activity reflecting an acquired internal model of a new tool. *Nature* 403: 192–195, 2000.

Jayaram G, Tang B, Pallegadda R, Vasudevan EV, Celnik P, Bastian A. Modulating locomotor adaptation with cerebellar simulation. *J Neurophysiol* 107: 2950–2957, 2012.

Kawato M, Furukawa K, Suzuki R. A hierarchical neural-network model for control and learning of voluntary movement. *Biol Cybern* 57: 169–185, 1987.

Knutsson E. Gait control in hemiparesis. *Scand J Rehabil Med* 13: 101–108, 1981.

Lam T, Wolstenholme C, Yang JF. How do infants adapt to loading of the limb during the swing phase of stepping? *J Neurophysiol* 89: 1920–1928, 2003.

Lam T, Anderschitz M, Dietz V. Contribution of feedback and feedforward strategies to locomotor adaptations. *J Neurophysiol* 95: 766–773, 2006.

Malone LA, Bastian AJ. Thinking about walking: effects of conscious correction versus distraction on locomotor adaptation. *J Neurophysiol* 103: 1954–1962, 2010.

Morton SM, Bastian AJ. Cerebellar contributions to locomotor adaptations during splitbelt treadmill walking. *J Neurosci* 26: 9107–9116, 2006.

Musselman KE, Patrick SK, Vasudevan EV, Bastian AJ, Yang JF. Unique characteristics of motor adaptation during walking in young children. *J Neurophysiol* 105: 2195–2203, 2011.

Nakazawa K, Kawashima N, Akai M, Yano H. On the reflex co-activation of ankle flexor and extensor muscles induced by a sudden drop of support surface during walking in humans. *J Appl Physiol* 94: 604–611, 2004.

Prokop T, Berger W, Zijlstra W, Dietz V. Adaptational and learning processes during human split-belt locomotion: interaction between central mechanisms and afferent input. *Exp Brain Res* 106: 449–456, 1995.

Reisman DS, Block HJ, Bastian AJ. Interlimb coordination during locomotion: what can be adapted and stored? *J Neurophysiol* 94: 2403–2415, 2005.

Reisman DS, Wityk R, Silver K, Bastian AJ. Locomotor adaptation on a split-belt treadmill can improve walking symmetry poststroke. *Brain* 130: 1861–72, 2007.

Reisman DS, Wityk R, Silver K, Bastian AJ. Split-belt treadmill adaptation transfers to overground walking in persons poststroke. *Neurorehabil Neural Repair* 23: 735–744, 2009.

Reisman DS, McLean H, Bastian AJ. Split-belt treadmill training poststroke: a case study. *J Neurol Phys Ther* 34: 202–207, 2010.

Shadmehr R, Mussa-Ivaldi FA. Adaptive representation of dynamics during learning of a motor task. *J Neurosci* 14: 3208–3224, 1994.

Sinkjaer T, Andersen JB, Larsen B. Soleus stretch reflex modulation during gait in humans. *J Neurophysiol* 76: 1112–1120, 1996.

Torres-Oviedo G, Bastian AJ. Seeing is believing: effects of visual contextual cues on learning and transfer of locomotor adaptation. *J Neurosci* 30: 17015–17022, 2010.

Vasudevan EV, Bastian AJ. Split-belt treadmill adaptation shows different functional networks for fast and slow human walking. *J Neurophysiol* 103: 183–191, 2010.

Vasudevan EV, Torres-Oviedo G, Morton SM, Yang JF, Bastian AJ. Younger is not always better: development of locomotor adaptation from childhood to adulthood. *J Neurosci* 31: 3055–3065, 2011.

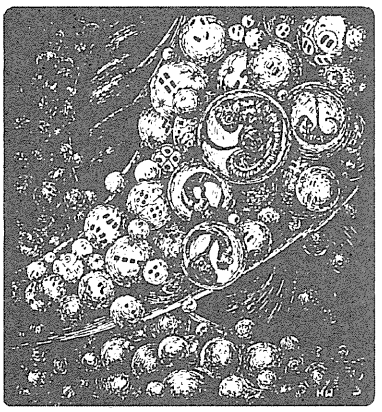

Chikuda et al. Trials 2013, 14:245
http://www.trialsjournal.com/content/14/1/245

TRIALS

STUDY PROTOCOL Open Access

Optimal treatment for Spinal Cord Injury associated with cervical canal Stenosis (OSCIS): a study protocol for a randomized controlled trial comparing early versus delayed surgery

Hirotaka Chikuda[1*], Hiroshi Ohtsu[2], Toru Ogata[4], Shurei Sugita[1], Masahiko Sumitani[3], Yurie Koyama[1], Morio Matsumoto[5], Yoshiaki Toyama[5] and on behalf of the OSCIS investigators

Abstract

Background: The optimal management of acute cervical spinal cord injury (SCI) associated with preexisting canal stenosis remains to be established. The objective of this study is to examine whether early surgical decompression (within 24 hours after admission) would result in greater improvement in motor function compared with delayed surgery (later than two weeks) in cervical SCI patients presenting with canal stenosis, but without bony injury.

Methods/design: OSCIS is a randomized, controlled, parallel-group, assessor-blinded, multicenter trial. We will recruit 100 cervical SCI patients who are admitted within 48 hours of injury (aged 20 to 79 years; without fractures or dislocations; American Spinal Injury Association (ASIA) grade C; preexisting spinal canal stenosis). Patients will be enrolled from 36 participating hospitals across Japan and randomly allocated in a 1:1 ratio to either early surgical decompression (within 24 hours after admission) or delayed surgery following at least two weeks of conservative treatment. The primary outcomes include: 1) the change from baseline to one year in the ASIA motor score; 2) the total score of the Spinal Cord Independence Measure and 3) the proportion of patients who are able to walk without human assistance. The secondary outcomes are: 1) the health-related quality of life as measured by the Medical Outcomes Study Short Form 36 and the EuroQol 5 Dimension; 2) the Neuropathic Pain Symptom Inventory and 3) the walking status as evaluated with the Walking Index for Spinal Cord Injury II. The analysis will be on an intention-to-treat basis. The primary analysis will be a comparison of the primary and secondary outcomes one year after the injury.

Discussion: The results of this study will provide evidence of the potential benefit of early surgical decompression compared to the current 'watch and wait' strategy.

Trial registration: UMIN000006780; NCT01485458

Keywords: Spinal cord injury, Surgery, Timing, Canal stenosis, Ossification of the posterior longitudinal ligament, Spondylosis, Spinal fracture, Bone injury

* Correspondence: chikuda-tky@umin.ac.jp
[1]Department of Orthopaedic Surgery, Faculty of Medicine, The University of Tokyo, 7-3-1 Hongo, Bunkyo-ku, Tokyo 113-8655, Japan
Full list of author information is available at the end of the article

Background

Acute cervical spinal cord injury (SCI) is one of the most devastating conditions, and can lead to paralysis, sensory impairment and bowel, bladder and sexual dysfunction. In addition, patients frequently suffer from intractable pain caused by neural damage. Individuals with cervical canal stenosis are known to develop cervical SCI even after minor trauma. Cervical canal stenosis may be congenital, but often results from degenerative conditions, such as spondylosis. The SCI patients with canal stenosis are mostly elderly, and usually present with incomplete SCI without bone injury, such as spinal fracture or dislocation. This subgroup of patients has been steadily increasing as the society ages and currently accounts for over 60% of cervical SCIs in Japan [1].

The clinical outcome of patients with incomplete SCI has been considered to be favorable, since patients usually show spontaneous neurologic recovery to some extent. However, the neurological prognosis varies greatly among patients; about half of ASIA C patients remain non-ambulatory six months after the injury [2]. In particular, the clinical outcomes of elderly patients are often suboptimal [3,4]. Therefore, a therapeutic option that leads to a better clinical outcome is urgently needed.

Controversy exists with regard to the efficacy of surgical decompression in the treatment of cervical SCI with preexisting canal stenosis [5,6]. The role of surgery remain unclear, especially in the absence of instability of the cervical spine [7], thus resulting in a significant difference in practice between institutions. A common approach to treating these patients has been to rule out acute instability and then observe the patients' spontaneous neurological recovery until they achieve a neurological plateau, and only then consider the possibility of surgical decompression, weeks after the initial injury [6]. Our previous retrospective multicenter study showed that the time from injury to surgery was approximately two weeks (median 13.5 days) [8].

The main drawback of this 'watch and wait' strategy is that a potential therapeutic window in the acute phase might be missed. The current concept of the pathophysiology of SCI classifies the spinal damage into two stages: primary injury and secondary injury [9]. The primary injury results from the mechanical forces delivered to the spinal cord at the time of the trauma. Secondary injury is a cascade of pathophysiological events including edema, ischemia, inflammation and apoptosis following the initial impact, which develops within minutes to hours following the trauma. There is a growing body of evidence from preclinical or animal studies that early surgical decompression alleviates 'secondary injury' and thus results in enhanced neurological and functional recovery [5].

Although numerous studies have been performed to examine the potential benefit of early surgery, the results of these prior clinical studies were mixed, and failed to provide robust support for the hypothesis that early surgery leads to improved outcomes. One small randomized trial of 42 patients showed no benefit to early (< 72 hours) decompression [10]. On the other hand, a meta-analysis of case series showed that early (< 24 hours) decompression was associated with better outcomes compared to both delayed (> 24 hours) and conservative treatment [11]. The results of STASCIS, one of the largest prospective studies of 313 patients, were also in favor of early surgery [12]. The authors of that study reported that early surgery, within 24 hours after injury, is associated with an improved neurological outcome, defined as at least a two grade ASIA Impairment Scale (AIS) improvement at the six-month follow-up examination. However, the difference in the chance of experiencing a one grade AIS improvement between early versus late surgery was not statistically significant.

With such conflicting information in the literature and a lack of high-quality evidence, it remains unclear whether early surgical decompression would result in better neurological and functional recovery. To address this issue, we launched the OSCIS study (Optimal treatment for Spinal Cord Injury associated with cervical canal Stenosis), a randomized, controlled, multicenter trial, in which we will compare the two strategies: early surgery within 24 hours after admission and delayed surgery following at least two weeks of conservative treatment.

Methods/design

Trial design

The OSCIS study is a randomized, controlled, parallel-group, assessor-blinded, multicenter study. Patients will be randomly allocated to undergo either early surgery or delayed surgery. The aim of this study is to test the hypothesis that early surgery (within 24 hours after admission) will lead to greater improvements in the motor function compared to delayed surgery (later than two weeks after injury) in patients with acute cervical SCI associated with canal stenosis. The flowchart shown in Figure 1 provides a visual description of the study.

Participants

Subjects will be recruited from 36 hospitals in Japan. The list of the participating hospitals with approval from local ethical boards is available as Additional file 1. We will screen all patients with acute traumatic cervical spinal cord injury (at C5 or below) who are admitted to one of the institutions within 48 hours after the injury. The diagnosis of cervical spinal cord injury will be made on the patient's history, including physical and neurological examinations, and the results of imaging studies,

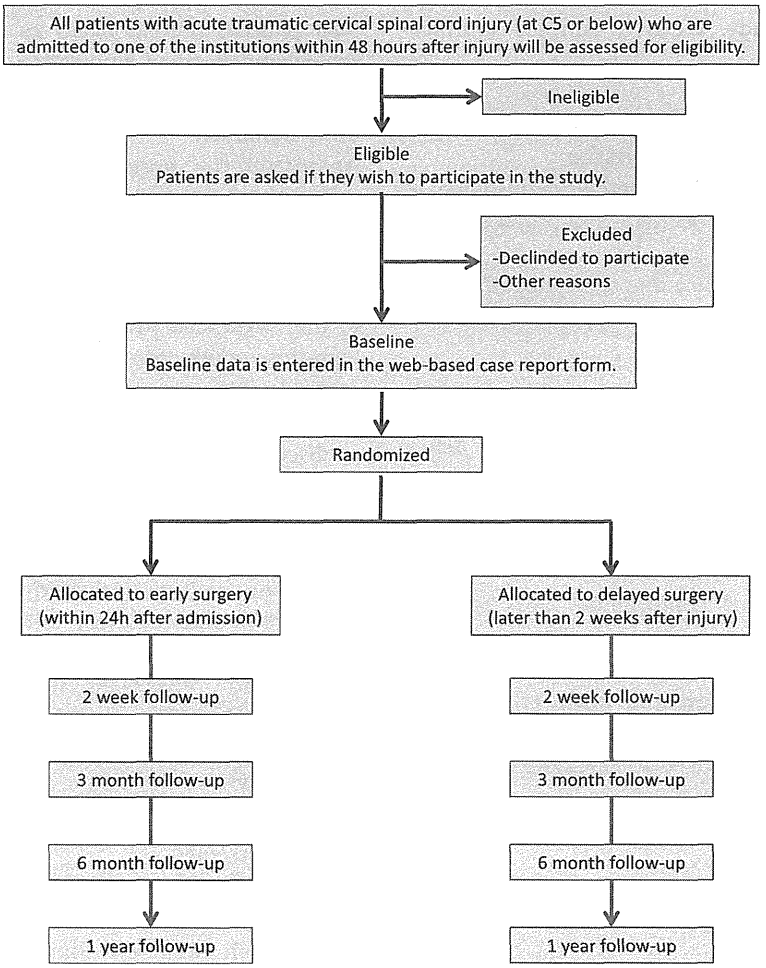

Figure 1 Study flowchart.

including plain radiographs, magnetic resonance imaging (MRI) and computed tomography (CT).

Inclusion criteria

Subjects will be eligible for inclusion if they satisfy the following inclusion criteria:

- aged 20 to 79 years
- without bone injury (spinal fracture or dislocation)
- American Spinal Injury Association (ASIA) impairment Grade C
- cervical canal stenosis due to preexisting conditions, such as spondylosis and ossification of the posterior longitudinal ligament (OPLL)

The presence of cervical canal stenosis will be confirmed by physicians based on the MRI findings obtained on admission. The presence of OPLL will be determined by using plain radiographs or CT. The thickness of the OPLL must be 20% or more of the spinal canal.

Exclusion criteria

Subjects will be excluded from enrollment if they meet any of the following conditions:

- unstable medical status
- unable to undergo surgery within 24 hours after admission
- impaired consciousness or mental disorder that precludes neurological examination
- difficulty in obtaining informed consent in Japanese

Randomization

We will adopt the web-based allocation system using the University Medical Information Network (UMIN), which is one of the data centers that run as a public institution in Japan. By entering the information about the patient, investigators will be able to know the allocation results immediately.

The allocation table, which was created by stratified block randomized by the trial statistician, is registered in

the UMIN. The block size is concealed to all investigators involved in this study. We have adopted stratification factors as follows:

- the presence of ossification of the posterior longitudinal ligament (OPLL) (yes/no)
- implementation of high-dose methylprednisolone treatment according to the NASCIS2 protocol (yes/no)
- preexisting gait disturbance due to myelopathy
- degree of canal compromise (50% or more/less than 50% canal compromise)

Preexisting gait disturbance due to myelopathy will be determined by the attending spine surgeon before randomization, based on thorough patients' history and available medical record. Gait disturbance attributable to other causes (for example, trauma, osteoarthritis, and paralysis after stroke) will be excluded.

Presence of severe canal compromise (50% or more canal compromise) will be assessed by the attending spine surgeon based on mid-sagittal MR images obtained at admission. For patients presented with OPLL, mid-sagittal reconstruction CT images or plain radiographs of the cervical spine will be used to calculate the degree of canal compromise.

Interventions

Patients will be randomly allocated to undergo either early surgery or delayed surgery.

Early surgery

Patients allocated to early surgery will undergo surgery within 24 hours after admission. The time when they enter the operating room will be used as a reference. The principal goal of surgery is to achieve decompression of the spinal cord. The choice of anterior or posterior approach will be left to the surgeon's discretion. The use of spinal instrumentation will be permitted when needed. The surgery will be performed by or under supervision of a board-certified orthopedic surgeon. The details of the surgical treatment and any perioperative adverse events will be recorded in a web-based predefined form. All patients will receive intensive rehabilitation tailored to the individual and injury-specific factors immediately after surgery.

Delayed surgery

Patients allocated to the delayed surgery group will receive conservative treatment consisting of early mobilization and intensive rehabilitation for at least two weeks after the injury. Surgical decompression will be performed by the same team as in the early surgery group at any time later than two weeks after the injury when the physician thinks the timing is appropriate. Physicians will be allowed to treat patients non-surgically as long as the patients can achieve independent ambulation.

Other treatments

Apart from the surgical management, all patients will receive appropriate medical support, including permissive or induced hypertensive therapy (mean blood pressure > 85 mmHg) [13]. High-dose methylprednisolone will be used per the discretion of the treatment team according to the NASCIS-2 protocol [1,14,15]. The use or lack of high-dose methylprednisolone must be determined and entered into the web-based database prior to the randomization. Physicians will not be allowed to change or discontinue the administration of methylprednisolone after randomization.

Primary and secondary outcomes

Participants will be evaluated two weeks, three months, six months and one year after randomization. Table 1 provides an overview of the outcomes that will be used in this study. Physicians and research nurses who are not involved in the patient's care will assess the outcome at each follow-up examination before the patients see their doctors.

Primary outcomes

The primary outcome is a recovery in motor function one year after injury. The assessment will include: 1) the change from baseline to one year after the admission in the ASIA motor score; 2) the total score of the Spinal Cord Independence Measure (SCIM) version 3 and 3) the proportion of patients who regained the ability to walk 100 meters without human assistance.

The ASIA motor score is a 100-point score based on ten pairs of key muscles, each given a five point rating. The SCIM is a validated 100-point disability scale developed specifically for patients with SCI, with an emphasis on daily tasks grouped into three subscales: self-care (20 points), respiration and sphincter management (40 points) and mobility (40 points) [16-18].

Secondary outcomes

The secondary outcomes will include: 1) the health-related quality of life as measured by the Medical Outcomes Study Short Form 36 (SF-36) [19,20] and the EuroQol 5 Dimension (EQ-5D) [21]; 2) the neuropathic pain at the injured level and below as assessed by the Neuropathic Pain Symptom Inventory (NPSI) [22] and 3) the walking status as evaluated with the Walking Index for Spinal Cord Injury (WISCI) II [23].

The scores on the SF-36 will be used as a generic measure of the patient health status. The SF-36 comprises eight

Table 1 The timeline of the outcome measures to be collected

		Follow-up			
	Admission	2 weeks	3 months	6 months	1 year
Visit	X[a]	X	X	X	X
Informed consent	X[a]				
Baseline clinical characteristics	X[a]				
Blood analyses	X[a]	X	X	X	X
Magnetic resonance imaging	X[a]				X
Computed tomography	X[a]				
Plain radiographs	X[a]	X			X
Neurological assessment including the ASIA motor score and ASIA impairment scale	X[a]	X	X	X	X
Evaluation of adverse events					
SCIM version 3		X	X	X	X
WISCI II		X			X
SF-36		X			X
EQ-5D		X	X	X	X
NPSI		X			X

X[a]: obtained prior to enrollment; ASIA: American Spinal Injury Association; EQ-5D: EuroQol 5 Dimension; NPSI, Neuropathic Pain Symptom Inventory; SCIM: Spinal Cord Independence Measure; SF-36: Medical Outcomes Study Short Form 36; WISCI: Walking Index for Spinal Cord Injury.

single subscale scores associated with physical and mental health.

The NPSI is a self-questionnaire specifically designed to evaluate the different symptoms of neuropathic pain. It includes 12 items, each of which is quantified on a (0 to 10) numerical scale. The pain associated with SCI is classified into two categories: at-level pain and below-level pain. Participants will be asked to complete the NPSI separately for pain in the upper extremities (at-level pain) and in the trunk and lower extremities (below-level pain). The WISCI II is a valid 21-level hierarchical scale of walking based on physical assistance, the need for braces and devices, with an ordinal range from 0 (unable to walk) to 20 (walking without assistance for at least 10 meters).

Adverse events

The occurrence of pre-specified adverse events will be also assessed. Adverse events will be gathered from patients themselves and from the patient record review. The *a priori* defined adverse events are: worsening of paralysis in the upper extremities, worsening of paralysis in the lower extremities, reoperation, use of a respirator (more than one week), tracheostomy, sepsis, pneumonia, acute respiratory distress syndrome, atelectasis, other respiratory complications, wound infection (superficial), wound infection (deep), urinary tract infection, other infections, gastrointestinal bleeding, peptic ulcer, ileus, acute myocardial infarction, other cardiac events, pulmonary embolism, cerebrovascular complication, liver dysfunction/disease, renal dysfunction/disease, delirium, depression, other complications and death.

Sample size

For this exploratory trial, the sample size was determined primarily based on feasibility. We assumed that it is feasible to enroll approximately 100 patients (50 patients per group) during the planned study period. As there is no valid data to indicate the optimal endpoint to evaluate the neurological and functional recovery of SCI patients, we selected three candidate endpoints as the primary endpoint: 1) the change from the baseline to one year after the admission in the ASIA motor score; 2) the proportion of patients who regained the ability to walk 100 meters without human assistance and 3) the total score of the Spinal Cord Independence Measure (SCIM) version 3.

We need 45 patients per group when the difference to be detected in the ASIA motor score between the groups is 12 points and the common standard deviation is 20. Additionally, we expect that the percentage of ambulatory patients one year after the injury will increase from 50% to 80%. To detect this difference, we need 39 patients for each group. With regard to the SCIM, there are few data that can be used as a basis for sample size calculation. For the reasons above, we set the sample size to be 50 patients per group. All calculations assume an 80% power at a two-tailed significance level of 0.05.

Statistical methods

All analyses will be based on an intention-to-treat principal, and will be performed with two-sided *P*-values considered significant when they are below 0.05. For a detailed analysis, the statistician will make a statistical analysis plan before the data lock, as indicated below:

1) Primary endpoint:
   - ASIA motor score
     Calculate the difference one year after the baseline, and compare the two groups using a *t*-test
   - The proportion of patients who regained the ability to walk
     Calculate the rate of patients who can walk one year after the baseline, and compare the two groups using the chi-square test
   - SCIM
     Compare the differences in the SCIM after one year.

2) Secondary endpoint:
   Compare the differences in the WISCI II, SF-36 and EQ-5D. For the SF-36, we plan to use only the total points, and not to compare each domain.
3) Safety:
   We will compare the rates of adverse events between the groups. In particular, in patients that are moved out of the surgical standby group, we will compare the ratio of the occurrence of adverse events with those in the patients in the early operation group.

Planned subgroup analyses

Predefined subgroup analyses will be performed in patients with or without OPLL. These will include high-dose methylprednisolone treatment, preexisting gait disturbance and severe canal compromise (> 50% canal compromise). Based on our previous study, we hypothesize that early surgical decompression will be beneficial in patients with preexisting gait disturbance and those with severe canal compromise.

Ethical issues

The study protocol was approved by the local ethics committees of all participating hospitals and will be done in accordance with the Declaration of Helsinki. The study will be overseen by an independent safety monitoring board. All participants will give written informed consent before entry.

Ethical approval was obtained from all participating hospitals. The results will be disseminated via the usual scientific forums, including peer-reviewed publications and presentations at international conferences.

Discussion

Despite intensive basic and clinical research, an effective treatment for cervical SCI has not been established. In the presence of preexisting canal stenosis, the role of surgical decompression and its optimal timing continue to be subjects of intense debate. Addressing the issue of the timing of surgical intervention is critical in that, if the timing of surgery has no effect on the patient's outcome, then all patients can initially be treated non-surgically and surgery can be delayed for weeks or even months after the injury without compromising the patient's recovery [6]. On the other hand, if early surgical decompression is proven to be beneficial, drastic changes in the medical service system, including logistics, should be made to ensure that all SCI patients receive early surgery.

In conducting clinical studies on SCI, the heterogeneity of the study population can be a major obstacle, especially in the acute phase. SCI patients vary greatly in the severity of paralysis and neurological prognosis. Clinical studies including patients with various degrees of neurological injury may have insufficient power. Therefore, in this study, we will focus on patients with ASIA C status. In a recent review, the consensus of experts was that it is reasonable to consider early surgical decompression in patients with profound neurologic deficit (ASIA C) and spinal canal stenosis without fracture or instability. On the other hand, those with a less severe deficit (ASIA D) can be treated with initial observation with surgery potentially performed at a later date [6]. We will exclude patients with ASIA B status, because these patients are often difficult to distinguish from ASIA A patients at the time of admission.

The information available regarding the window of opportunity or therapeutic window in human SCI is imprecise [24] and the definition of 'early surgery' has not yet been well established. Although the ideal cutoff time at which surgery provides potential neuroprotection is not known, the most intensively investigated times in the prior studies were 24 and 72 hours. In this study, we have adopted a cutoff at twenty-two hours after admission mainly for practical and logistic reasons. Twenty-four hours after admission is considered to be necessary and sufficient to safely perform the initial evaluation of patients and summon the operating team for emergency surgery. In this study, we adopted the time of admission as a reference, since the time of injury sometimes remains conjectural.

The OSCIS study is designed to provide evidence of the potential benefit of early surgical decompression over a wait-and-see strategy. We believe that the results of this trial will have a substantial impact on the management of cervical SCI.

Trial status

The trial was registered in the UMIN register on 1 December, 2011. The first patient was randomized on 3 December, 2011. The trial is currently open for recruitment.

Additional file

Additional file 1: List of participating hospitals with approval from local ethical boards (as of 6 August, 2013).

Abbreviations

AIS: ASIA Impairment Scale; ASIA: American Spinal Injury Association; CT: Computed tomography; EQ-5D: EuroQol 5 Dimension; MRI: Magnetic resonance imaging; OPLL: Ossification of the posterior longitudinal ligament; SCI: Spinal cord injury; SCIM: Spinal Cord Independence Measure; SF-36: Medical Outcomes Study Short Form 36; UMIN: University Medical Information Network; WISCI: Walking Index for Spinal Cord Injury.

Competing interests

The authors declare that they have no competing interests.

Authors' contributions

HC, HO, TO, SS, MS, MM, and YT participated in the conception and design of the study. YK will participate in the monitoring and quality control of the data. HC drafted the manuscript. All authors read, commented on and approved the manuscript.

Acknowledgement

This study is being performed with the aid of the Investigation Committee on the Ossification of the Spinal Ligaments of the Japanese Ministry of Health, Labor and Welfare. This study is also supported by the JOA-Subsidized Science Project Research 2012-2.

Author details

[1]Department of Orthopaedic Surgery, Faculty of Medicine, The University of Tokyo, 7-3-1 Hongo, Bunkyo-ku, Tokyo 113-8655, Japan. [2]Department of Clinical Trial Data Management, Graduate School of Medicine, The University of Tokyo, 7-3-1 Hongo, Bunkyo-ku, Tokyo 113-8655, Japan. [3]Department of Medical Engineering, Faculty of Medicine, The University of Tokyo, 7-3-1 Hongo, Bunkyo-ku, Tokyo 113-8655, Japan. [4]Rehabilitation for the Movement Functions, Research Institute, National Rehabilitation Center for Persons with Disabilities, Saitama 359-8555, Japan. [5]Department of Orthopaedic Surgery, School of Medicine, Keio University, 35 Shinanomachi, Shinjuku, Tokyo 160-0016, Japan.

Received: 27 April 2013 Accepted: 31 July 2013
Published: 7 August 2013

References

1. Chikuda H, Yasunaga H, Takeshita K, Horiguchi H, Kawaguchi H, Ohe K, Fushimi K, Tanaka S: **Mortality and morbidity after high-dose methylprednisolone treatment in patients with acute cervical spinal cord injury: a propensity-matched analysis using a nationwide administrative database.** *Emerg Med J* 2013. doi:10.1136/emermed-2012-202058.
2. Pouw MH, van Middendorp JJ, van Kampen A, Curt A, van de Meent H, Hosman AJ: **Diagnostic criteria of traumatic central cord syndrome. Part 3: descriptive analyses of neurological and functional outcomes in a prospective cohort of traumatic motor incomplete tetraplegics.** *Spinal Cord* 2011, **49**:614–622.
3. Burns SP, Golding DG, Rolle WA Jr, Graziani V, Ditunno JF Jr: **Recovery of ambulation in motor-incomplete tetraplegia.** *Arch Phys Med Rehabil* 1997, **78**:1169–1172.
4. Foo D: **Spinal cord injury in forty-four patients with cervical spondylosis.** *Paraplegia* 1986, **24**:301–306.
5. Cadotte DW, Fehlings M: **Role of early decompression for spinal cord injury.** In *Controversies in spine surgery: best evidence recommendations.* Edited by Vaccaro A, Eck J. New York: Thieme; 2010:86–92.
6. Lenehan B, Fisher CG, Vaccaro A, Fehlings M, Aarabi B, Dvorak MF: **The urgency of surgical decompression in acute central cord injuries with spondylosis and without instability.** *Spine (Phila Pa 1976)* 2010, **35**:S180–186.
7. Kawano O, Ueta T, Shiba K, Iwamoto Y: **Outcome of decompression surgery for cervical spinal cord injury without bone and disc injury in patients with spinal cord compression: a multicenter prospective study.** *Spinal Cord* 2010, **48**:548–553.
8. Chikuda H, Seichi A, Takeshita K, Matsunaga S, Watanabe M, Nakagawa Y, Oshima K, Sasao Y, Tokuhashi Y, Nakahara S, *et al*: **Acute cervical spinal cord injury complicated by preexisting ossification of the posterior longitudinal ligament: a multicenter study.** *Spine (Phila Pa 1976)* 2011, **36**:1453–1458.
9. Steinmets MP, Anderson PA, Patel R, Resnick DK: **Anatomy and pathophysiology of spinal cord injury.** In *Atlas of spine trauma: adult and pediatric.* Edited by Kim DH, Ludwig SC, Vaccaro A, Chang J. Philadelphia, Pennsylvania: Saunders; 2008:11–20.
10. Vaccaro AR, Daugherty RJ, Sheehan TP, Dante SJ, Cotler JM, Balderston RA, Herbison GJ, Northrup BE: **Neurologic outcome of early versus late surgery for cervical spinal cord injury.** *Spine (Phila Pa 1976)* 1997, **22**:2609–2613.
11. La Rosa G, Conti A, Cardali S, Cacciola F, Tomasello F: **Does early decompression improve neurological outcome of spinal cord injured patients? Appraisal of the literature using a meta-analytical approach.** *Spinal Cord* 2004, **42**:503–512.
12. Fehlings MG, Vaccaro A, Wilson JR, Singh A, Cadotte WD, Harrop JS, Aarabi B, Shaffrey C, Dvorak M, Fisher C, *et al*: **Early versus delayed decompression for traumatic cervical spinal cord injury: results of the Surgical Timing in Acute Spinal Cord Injury Study (STASCIS).** *PLoS One* 2012, **7**:e32037.
13. Vale FL, Burns J, Jackson AB, Hadley MN: **Combined medical and surgical treatment after acute spinal cord injury: results of a prospective pilot study to assess the merits of aggressive medical resuscitation and blood pressure management.** *J Neurosurg* 1997, **87**:239–246.
14. Bracken MB, Shepard MJ, Collins WF, Holford TR, Young W, Baskin DS, Eisenberg HM, Flamm E, Leo-Summers L, Maroon J, *et al*: **A randomized, controlled trial of methylprednisolone or naloxone in the treatment of acute spinal-cord injury. Results of the Second National Acute Spinal Cord Injury Study.** *N Engl J Med* 1990, **322**:1405–1411.
15. Ito Y, Sugimoto Y, Tomioka M, Kai N, Tanaka M: **Does high dose methylprednisolone sodium succinate really improve neurological status in patient with acute cervical cord injury?: a prospective study about neurological recovery and early complications.** *Spine (Phila Pa 1976)* 2009, **34**:2121–2124.
16. Bluvshtein V, Front L, Itzkovich M, Aidinoff E, Gelernter I, Hart J, Biering-Soerensen F, Weeks C, Laramee MT, Craven C, *et al*: **SCIM III is reliable and valid in a separate analysis for traumatic spinal cord lesions.** *Spinal Cord* 2011, **49**:292–296.
17. Catz A, Itzkovich M, Agranov E, Ring H, Tamir A: **SCIM - spinal cord independence measure: a new disability scale for patients with spinal cord lesions.** *Spinal Cord* 1997, **35**:850–856.
18. Itzkovich M, Gelernter I, Biering-Sorensen F, Weeks C, Laramee MT, Craven BC, Tonack M, Hitzig SL, Glaser E, Zeilig G, *et al*: **The Spinal Cord Independence Measure (SCIM) version III: reliability and validity in a multi-center international study.** *Disabil Rehabil* 2007, **29**:1926–1933.
19. Fukuhara S, Bito S, Green J, Hsiao A, Kurokawa K: **Translation, adaptation, and validation of the SF-36 Health Survey for use in Japan.** *J Clin Epidemiol* 1998, **51**:1037–1044.
20. Ware JE Jr, Sherbourne CD: **The MOS 36-item short-form health survey (SF-36). I. Conceptual framework and item selection.** *Med Care* 1992, **30**:473–483.
21. The EuroQol Group: **EuroQol - a new facility for the measurement of health-related quality of life.** *Health Policy* 1990, **16**:199–208.
22. Bouhassira D, Attal N, Fermanian J, Alchaar H, Gautron M, Masquelier E, Rostaing S, Lanteri-Minet M, Collin E, Grisart J, *et al*: **Development and validation of the Neuropathic Pain Symptom Inventory.** *Pain* 2004, **108**:248–257.
23. Dittuno PL, Ditunno JF Jr: **Walking index for spinal cord injury (WISCI II): scale revision.** *Spinal Cord* 2001, **39**(12):654–656.
24. Tator CH: **Review of treatment trials in human spinal cord injury: issues, difficulties, and recommendations.** *Neurosurgery* 2006, **59**:957–982.

doi:10.1186/1745-6215-14-245
Cite this article as: Chikuda *et al.*: Optimal treatment for Spinal Cord Injury associated with cervical canal Stenosis (OSCIS): a study protocol for a randomized controlled trial comparing early versus delayed surgery. *Trials* 2013 **14**:245.

Zhang et al. Molecular Brain 2014, 7:14
http://www.molecularbrain.com/content/7/1/14

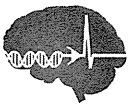

Molecular Brain

RESEARCH Open Access

Rewiring of regenerated axons by combining treadmill training with semaphorin3A inhibition

Liang Zhang[1,2,3†], Shinjiro Kaneko[1,4†], Kaoru Kikuchi[5], Akihiko Sano[5], Miho Maeda[5], Akiyoshi Kishino[5], Shinsuke Shibata[2], Masahiko Mukaino[3], Yoshiaki Toyama[1], Meigen Liu[3], Toru Kimura[5], Hideyuki Okano[2*†] and Masaya Nakamura[1*†]

Abstract

Background: Rats exhibit extremely limited motor function recovery after total transection of the spinal cord (SCT). We previously reported that SM-216289, a semaphorin3A inhibitor, enhanced axon regeneration and motor function recovery in SCT adult rats. However, these effects were limited because most regenerated axons likely do not connect to the right targets. Thus, rebuilding the appropriate connections for regenerated axons may enhance recovery. In this study, we combined semaphorin3A inhibitor treatment with extensive treadmill training to determine whether combined treatment would further enhance the "rewiring" of regenerated axons. In this study, which aimed for clinical applicability, we administered a newly developed, potent semaphorin3A inhibitor, SM-345431 (Vinaxanthone), using a novel drug delivery system that enables continuous drug delivery over the period of the experiment.

Results: Treatment with SM-345431 using this delivery system enhanced axon regeneration and produced significant, but limited, hindlimb motor function recovery. Although extensive treadmill training combined with SM-345431 administration did not further improve axon regeneration, hindlimb motor performance was restored, as evidenced by the significant improvement in the execution of plantar steps on a treadmill. In contrast, control SCT rats could not execute plantar steps at any point during the experimental period. Further analyses suggested that this strategy reinforced the wiring of central pattern generators in lumbar spinal circuits, which, in turn, led to enhanced motor function recovery (especially in extensor muscles).

Conclusions: This study highlights the importance of combining treatments that promote axon regeneration with specific and appropriate rehabilitations that promote rewiring for the treatment of spinal cord injury.

Keywords: Axonal regeneration, Semaphorin3A, Inhibitor, Rehabilitation, Rewiring, Drug delivery system

Background

Severe spinal cord injuries (SCI) in adult mammals result in various deficits throughout life. The limited capability of axons to regenerate in the central nervous system (CNS) is thought to be the main reason for these lasting deficits. Previous studies have suggested that both extrinsic and intrinsic factors in the CNS contribute to this incapacity for axonal regeneration [1-4]. Several distinct extrinsic molecules have been proposed to hinder axonal regeneration, including CNS myelin-associated proteins (MAG, Nogo, OMgp) [5-9], chondroitin sulphate proteoglycans [10,11], semaphorin3A [12,13] and RGM (repulsive guidance molecule) [14,15]. Neutralizing one (or several) of these molecules enhances axonal regeneration and results in some degree of functional recovery [10,16,17]. Until recently, it remained unknown whether neutralizing semaphorin3A would also lead to axonal regeneration and motor function recovery, in part because semaphorin3A deficiency is lethal [18]. Thus, we previously developed a selective and potent semaphorin3A inhibitor called SM-216289 [19] that selectively inhibits semaphorin3A signaling both *in vitro* and *in vivo* [20]. Administration of SM-216289 to adult rats after total spinal cord transection

* Correspondence: hidokano@a2.keio.jp; masa@a8.keio.jp
†Equal contributors
[2]Department of Physiology, Keio University School of Medicine, 35 Shinanomachi, Shinjuku, Tokyo 160-8582, Japan
[1]Department of Orthopedic Surgery, Keio University School of Medicine, 35 Shinanomachi, Shinjuku, Tokyo 160-8582, Japan
Full list of author information is available at the end of the article

(SCT) led to axonal regeneration and motor function recovery [20]. In addition, axonal regeneration and functional recovery have now been observed after several treatments that block 1 or more axonal growth inhibitors (including SM-216289). However, these effects are moderate at best, presumably because most of the regenerated axons do not connect with the correct targets [21]. Thus, rebuilding the appropriate connections of regenerated axons in lesioned spinal cords remains an important unresolved issue.

Body weight-supported treadmill training induces plastic changes in lesioned spinal cords and is useful for maximizing residual locomotor function after moderate SCI [22,23]. Furthermore, even after severe SCI, treadmill training partially improves hindlimb coordination [24] by inducing plasticity in specific spinal locomotor circuits called "central pattern generators" (CPGs). More specifically, these plastic changes have been shown to result in the recovery of plantar step walking in cats [25] and neonatal rats [26]. Furthermore, SCT adult rats partially recover plantar step walking when treadmill training is combined with other appropriate treatments, such as epidural electrical stimulation [27], pharmacological treatments [24] or cell transplantation [28]. Thus, with specific and appropriate rehabilitation, spinal cord CPGs can be reorganized, and functionally appropriate connections between CPGs and regenerated (or residual) axons can be rebuilt. Therefore, we hypothesized that extensive treadmill training would assist in the correct wiring of axons regenerated by semaphorin3A inhibitor treatment and that this rewiring may contribute to further motor functional recovery after SCT.

However, several issues, including drug delivery, remain to be resolved before semaphorin3A inhibitors can be used in the clinic. In an attempt to resolve these issues, we developed a novel selective semaphorin3A inhibitor, SM-345431 (Vinaxanthone), which demonstrates physicochemical properties equivalent to those of SM-216289 but also improvements that should allow for the development of a higher quality pharmaceutical product. Additionally, we developed a novel drug delivery system (DDS) utilizing a silicone sheet. With future clinical applications in mind, we chose to evaluate SM-345431 with this novel DDS. We observed that, consistent with our previous study [20], SM-345431 treatment enhanced axon regeneration and resulted in significant, but limited, hindlimb motor function recovery. Although extensive treadmill training with SM-345431 administration did not further improve axon regeneration, hindlimb motor performance was restored, as evidenced by the execution of plantar steps on a treadmill using a body support system (BSS). Moreover, immunohistological analysis suggested that SM-345431 administration with treadmill training reinforced the wiring of CPGs in lumbar spinal circuits and led to enhanced motor function recovery, especially in extensor muscles.

Results

Evaluation of a novel DDS and the activity of SM-345431 *in vitro*

In our previous study, we used an osmotic mini-pump to deliver the semaphorin3A inhibitor SM-216289 [20]. However, in clinical practice, this type of invasive drug delivery method is not ideal. Therefore, we developed a novel DDS that utilizes a silicone matrix to continuously deliver SM-345431 (a newly developed semaphorin3A inhibitor) intrathecally. We evaluated the drug release profile of SM-345431 in this new silicone matrix preparation and the potency of SM-345431-mediated semaphorin3A inhibition in vitro (Figure 1). SM-345431 exhibited semaphorin3A inhibiting activity with an IC50 of 0.1-0.2 μM in growth cone collapse assays using E8 chick and E14 rat dorsal root ganglia (DRG) (Figure 1A). When chick embryonic DRG explants and semaphorin3A-expressing COS7 cell aggregates (semaphorin3A-COS) were co-cultured in a collagen gel, the neurites of the DRG explants grew away from the semaphorin3A-COS, as shown in Figure 1B. However, when DRG explants and semaphorin3A-COS were co-cultured in the presence of SM-345431, radial extensions of the neurites were observed, which suggests that the chemo-repulsive effects of semaphorin3A were blocked by SM-345431 in a dose-dependent manner (Figure 1B). We also evaluated the selectivity of SM-345431 for semaphorin3A inhibition by examining the pharmacological profile of SM-345431 (Tables 1 and 2). As shown in these tables, the IC50 value for semaphorin3A inhibition was substantially lower than the other IC50s, which suggested that SM-345431 is a highly selective semaphorin3A inhibitor. To examine the semaphorin3A inhibiting activity of SM-345431 while it was being released from the silicone matrix (SM-345431-silicone), 1 mg of a silicone sheet containing 100 μg SM-345431 was placed into collagen gel cultures containing DRG explants and semaphorin3A-COS (Figure 1C). Assuming that 5% of the SM-345431 was released and uniformly diffused throughout the culture during the 2 days of incubation, the final concentration of SM-345431 was approximately 5 μM, which is a large enough dose to inhibit semaphorin3A activity. Radial neurite extension was observed in cultures with SM-345431-silicone but not in those with control silicone, indicating that semaphorin3A activity had been inhibited by SM-345431. We also measured the cumulative percentage of released doses of SM-345431 using this DDS over 2 months *in vitro* (Figure 1E) and found that this DDS released a constant dose of SM-345431 and was stable *in vitro*. When 7 mm × 5 mm × 0.3 mm sheets were used, the amount of drug release stabilized at approximately 10 μg/day after an initial peak of drug release that occurred over the first 2 days (Figure 1F). For the *in vivo* study, we trimmed the silicone sheet into 3 mm × 3 mm × 0.3 mm pieces to fit the injury site following SCT (Figure 1G-I).

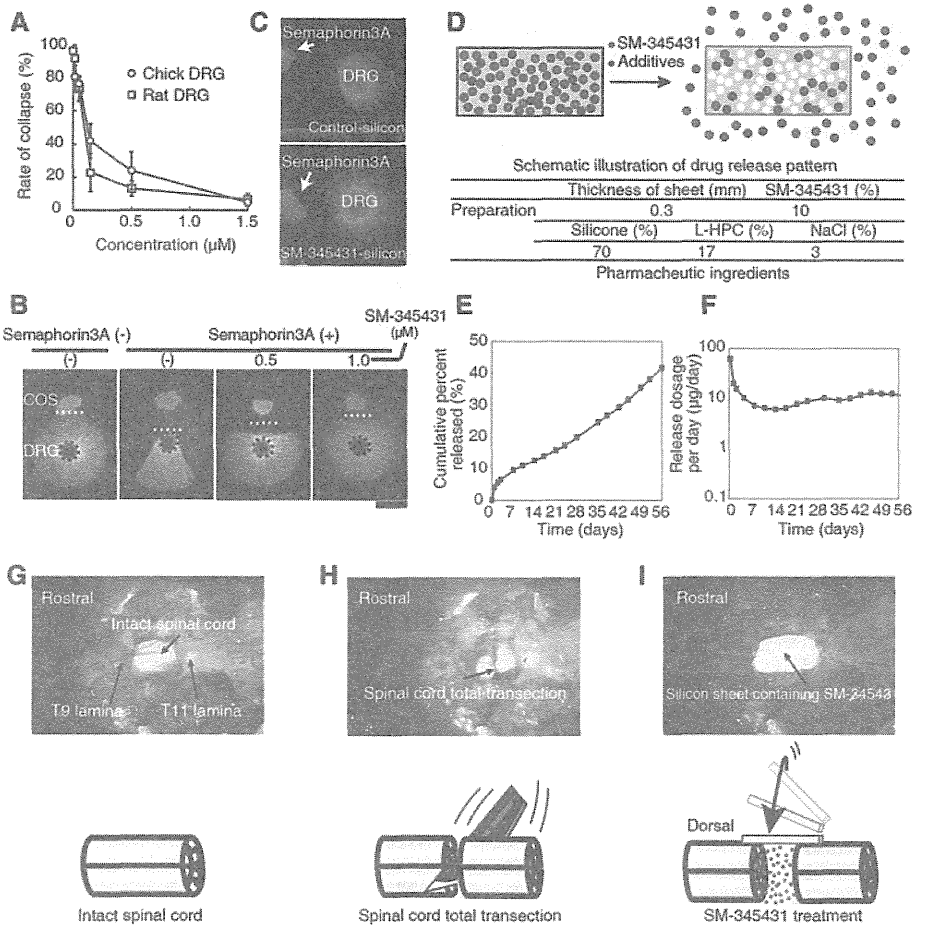

Figure 1 Preparation of the SM-345431 silicone DDS and *in vitro* release study. (A) Analysis of the inhibitory activity of SM-345431 in the growth cone collapse assay using E8 chick and E14 rat DRGs. **(B)** Collagen co-culture assay using E8 chick DRGs and semaphorin3A-expressing COS7 cell aggregates. **(C)** Pictures showing the effects of SM-345431-silicone or control-silicone in the collagen gel. **(D)** Schematic illustration of drug release from the matrix silicone preparation; the drug is dissolved in water, permeates into the preparation and is then released. The rate of water permeation into the silicone matrix is controlled by various additives, and the proportions of these additives included in the DDS control the variations in the drug release profile. The preparation used here contained the water-soluble additives listed in the table **(D)**. Stable and linear release of SM-345431 was observed for up to 2 months as shown in **(E)** and **(F)**. **(E, F)** SM-345431 release curve for the preparation. The linear cumulative percent release curve at 2 months **(E)** and the stable release dosage per day **(F)** are shown for the administration of SM-345431 using this novel DDS. **(G)** Exposed intact spinal cord. **(H)** Transected spinal cord. **(I)** The novel DDS we employed. A silicone sheet containing SM-345431 was placed onto the transected site of the spinal cord. The system allowed for stable and continuous release of the semaphorin3A inhibitor throughout the experimental period.

The release of SM-345431 (0.1 mg/mg loading 10%) *in vivo* was calculated as 0.5-0.7 μg/day, and this dose was similar to the dose of the semaphorin3A inhibitor (SM-216289) [19] that we administered using osmotic mini pumps in our previous study [20]. Therefore, the newly developed DDS allowed stable and continuous release of the newly developed, potent semaphorin3A inhibitor SM-345431.

SM-345431 delivery via the novel DDS enhanced axonal regeneration

To examine the regeneration of axons after SM-345431 treatment and SM-345431 treatment combined with extensive treadmill training, we evaluated axons in the injured spinal cord with immunostaining using antibodies against GAP43 and serotonin (5-HT) (Figure 2), GAP43 is widely used as a marker for regenerated axons. In both treatment groups, a marked increase in the number of GAP43-positive axons was observed at the epicenter of the injury (Figure 2D-F) and in the surrounding area (Figure 2G-I). Compared with the control group, the number of GAP43 axons was significantly increased in both the SM-345431 treatment group and the combined treatment group, especially at 1 mm caudal to the injury epicenter (Figure 2J). No significant difference was observed between the 2 treatment groups. Thus, administration of the semaphorin3A inhibitor SM-345431 using this DDS enhanced axonal

Table 1 Pharmacological profile of SM-345431 (part 1)

Enzymes	IC50 (μm)
Semaphorin	0.1-0.2
Matrix Metalloproteinase-1 (MMP-1)	>10
Matrix Metalloproteinase-7 (MMP-7)	10
Matrix Metalloproteinase-2 (MMP-2)	>10
Matrix Metalloproteinase-3 (MMP-3)	>10
Matrix Metalloproteinase-9 (MMP-9)	>10
Phospholipase PLA2-1	>10
Phospholipase PLC	>10
Caspase 1	>10
Caspase 3	>10
Caspase 6	>10
Caspase 7	>10
Caspase 8	>10
Protein Tyrosine Phosphatase, CD45	>10
Protein Tyrosine Phosphatase, PTP1B	>10
Protein Tyrosine Phosphatase, PTP1C	>10
Protein Tyrosine Phosphatase, T-Cell	>10
Sphingomyelinase, Neutral (N-SMase)	>10
Chemokine CCR1	>10
Chemokine CCR2B	>10
Chemokine CCR4	>10
Chemokine CCR5	>10
Chemokine CXCR2 (IL-8B)	>10
Glucocorticoid	>10
Interleukin IL-1	>10
Interleukin IL-2	>10
Interleukin IL-6	>10
Tumor Necrosis Factor (TNF), Non-selective	>10
Adhesion, fibronectin-mediated	>10
Adhesion, ICAM-1-Mediated	>10
Adhesion, VCAM-1-Mediated	>10
Cell proliferation, B-Cell+LPS	>10
Cell proliferation, T-Cell+Con A	>10
Mediator release, IL-1beta	>10
Mediator release, IFN-gamma	>10
Mediator release, IL-10	>10
Mediator release, IL-2	>10
Mediator release, IL-4	>10
Mediator release, IL-5	>10
Mediator release, IL-6	>10
Mediator release, TNF-alfa, PBML	>10
Transcription response, NF-AT	>10
Transcription response, NF-kB	>10

Summary of the IC50 values for binding assays of various receptors and ion channels, and IC50 values for the inhibition of various enzymes. The IC50 value for semaphorin3A inhibition was extremely low compared to that of the other factors.

Table 2 Pharmacological profile of SM-345431 (part 2)

Kinases	IC50 (μm)
CaMKII	>10
CDK5/p35	>10
cSRC	>10
EGFR	0.90
EphA2	>10
EphA4	0.80
EphB2	0.68
EphB4	>10
Fes	>10
FGFR1	>10
FGFR2	>10
FGFR3	0.77
FGFR4	0.64
Flt1	>10
Flt3	>10
Fyn	>10
GSK3α	2.46
GSK3β	>10
IGF-1R	>10
JAK3	>10
KDR	>10
MAPK2	>10
MEK1	>10
MEK4	>10
MKK6	>10
PAK2	>10
PAK4	>10
PKA	>10
PKBα	>10
PKBβ	>10
PKCγ	>10
ROCK-I	>10
ROCK-II	>10
ROCK-II	>10
SAPK2a	>10
TrkA	>10
TrkB	>10
PI 3-Kγ	>10

Summary of the IC50 values revealed by inhibition tests for various kinases. The data in Tables 1 and 2 suggest that SM-345431 was highly selective for semaphorin3A inhibition.

regeneration. However, no additional axonal regeneration was observed when SM-345431 treatment was combined with treadmill training.

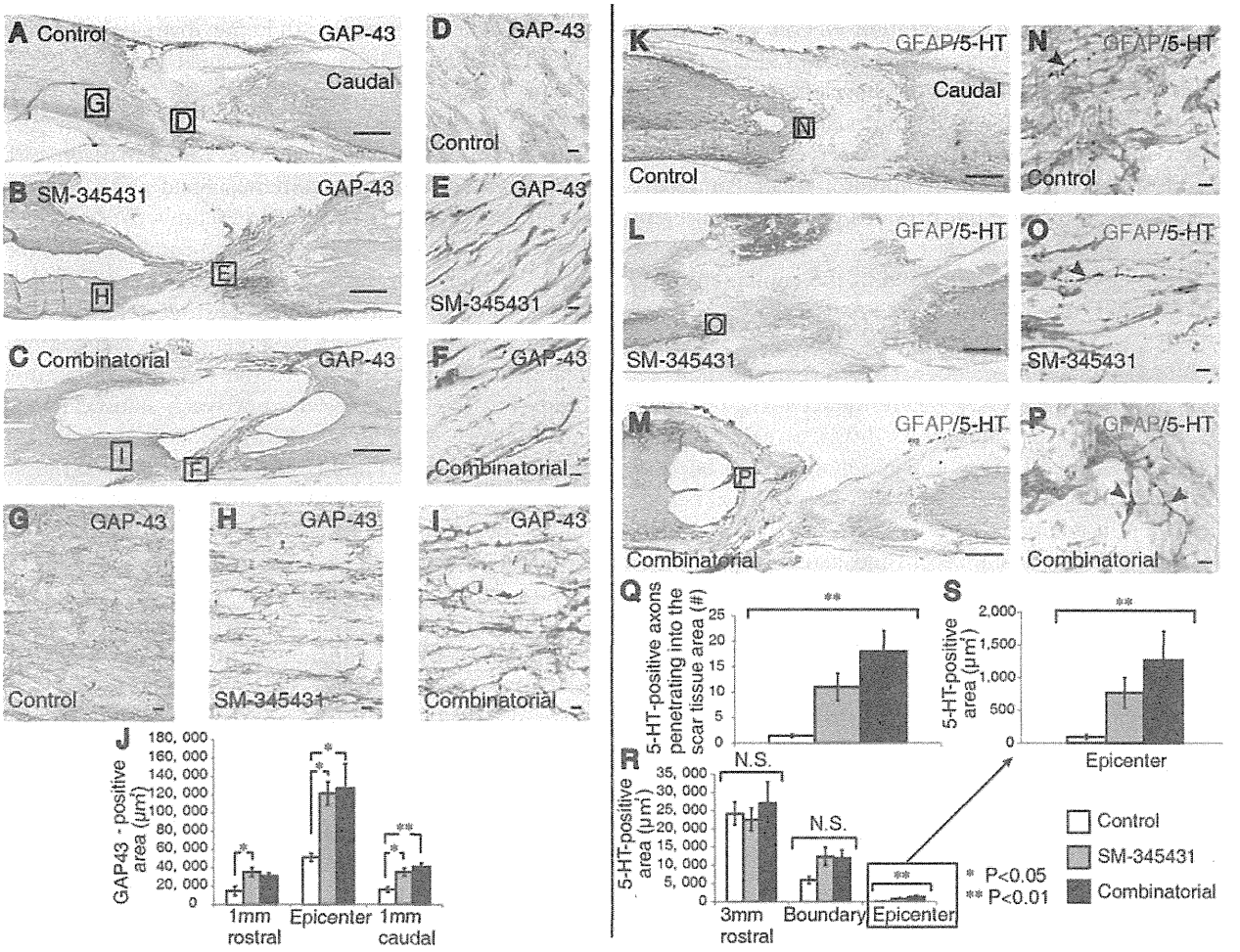

Figure 2 SM-345431 enhanced axonal regeneration *in vivo*, but combined treatment had only a limited effect on further axon regeneration. (A-I) Sagittal sections from SCT rats immunostained for GAP-43. Low-magnification images of the control **(A)**, SM-345431 **(B)** and combined treatment **(C)** groups. Scale bars = 500 μm. **(D-F)** Magnified images of the boxed areas shown in **A-C**. Scale bars = 10 μm. **(G-I)** Additional magnified images of the boxed areas shown in **A-C**. Scale bars = 10 μm. **(J)** Quantitative analysis of GAP-43-positive areas at 1 mm rostral to the lesion, 1 mm caudal to the lesion and at the epicenter of the lesion. Immunohistochemistry was performed using DAB with nickel enhancement. *P < 0.05, **P < 0.01. Statistical analyses were performed using one-way ANOVA and Bonferroni post hoc tests. Data are represented as the mean ± S.E.M. **(K-P)** Sagittal sections of SCT rats double-stained for 5-HT and GFAP. Scar tissue is outlined by GFAP staining, which also allowed for confirmation of total transection of the spinal cord in each animal. **(K-M)** Low-magnification images of the control **(K)**, SM-345431 **(L)** and combined treatment **(M)** groups. Scale bars = 500 μm. **(N-P)** Magnified images of the boxed areas shown in **K-M**. Scale bars = 10 μm. Arrowheads represent 5-HT-positive (serotonergic) axons. **(Q-S)** Quantitative analyses of 5-HT-positive axons that penetrated into the scar tissue. **(Q)** Quantitative analysis of the number of 5-HT-positive axons that penetrated into the lesion site. **(R,S)** Quantitative analysis of the 5-HT-positive area within the scar tissue area. Immunohistochemistry was performed by double-staining using DAB with or without nickel enhancement. The left side is rostral in all images. **P < 0.01. Statistical analyses were performed using a Kruskal-Wallis H test. Data represent the mean ± S.E.M.

The raphespinal tract axons, which can be detected by immunohistochemistry against serotonin (5-HT), contribute to functional locomotor control, and regeneration of these axons leads to substantial enhancement of motor function recovery [28]. Therefore, we also evaluated the regeneration of raphespinal tract axons using a GFAP antibody to delineate scar tissue at the injury site and a 5-HT antibody to visualize raphespinal axons. In control animals, 5-HT-positive axons were restricted to the area rostral to the transected site, and few 5HT-positive axons entered the GFAP-negative scar tissue area (Figure 2K,N). Interestingly, significantly more 5-HT-positive axons penetrated the GFAP-negative scar tissue area after SM-345431 treatment and combined treatment as compared to the control conditions (Figure 2K-S). Because we used a total transection model in this study, the 5-HT-positive axons that penetrated the GFAP-negative scar tissue in the treatment groups were regarded as regenerated axons (Figure 2L-P). Cortico-spinal tract (CST) axons are known to be incapable of regeneration after transection, even